Available online at www.sciencedirect.com
ScienceDirect
Journal of Sound and Vibration 297 (2006) 635–648
JOURNAL OF SOUND AND VIBRATION
www.elsevier.com/locate/jsvi

Influence of restrictor on stability of the rigid rotor–hybrid bearing system

Cheng Hsien Chen[a], Yuan Kang[b,*], Yeon-Pun Chang[b], Yea-Ping Wang[b], Hsing-Han Lee[b]

[a]*Department of Vehicle Engineering, Army Academy Taiwan, Republic of China*
[b]*Department of Mechanical Engineering, Chung Yuan Christian University, 200 Chung Pei Road, Chung Li, 32023 Taiwan, Republic of China*

Received 10 May 2005; received in revised form 6 April 2006; accepted 10 April 2006
Available online 15 June 2006

Abstract

This paper investigates the restriction effects of capillary and orifice on the stability of the rigid rotor–hybrid bearing system. The finite difference method and numerical integration are used to solve the Reynolds lubrication equations and static and dynamic performances of lubrication film, respectively, and the Routh–Hurwitz method is used to determine the stability threshold. The results reveal that the influence of stability threshold versus carrying load according to hybrid bearings with or without restrictors, as well as, shallow or deep recesses and various land-width ratios.

1. Introduction

The hybrid journal bearings have gained considerably, in many engineering applications such as precision machinery, since they combine the merits of hydrostatic and hydrodynamic bearings. Capillary and orifice are most commonly restrictors for hydrostatic and hybrid bearings because of simple manufacturing. Raimondi and Boyd [1] utilized experiment to yield the maximum load capacity at the optimal restriction parameters of capillary or orifice for hydrostatic bearings. Rowe and Chong [2] showed that the perturbation techniques contribute more efficient than disturbance method in computing the dynamic coefficients. Ghosh [3], Ghosh et al. [4], Ghosh and Viswanath [5] and Ghosh et al. [6,7] utilized the small perturbation method to evaluate static and dynamic coefficients of multirecessed hybrid bearings. Results indicated that the recess volume fluid compressibility would affect the dynamic characteristics of hybrid bearings in higher excited frequency range.

Cheng and Rowe [8] have claimed that the design of the restrictors becomes critical and must be undertaken in parallel with the bearing configuration. Braun et al. [9–11] studied recesses depth and feed-line problems of

*Corresponding author. Tel.: +886 3 2654315; fax: +886 3 2654351.
E-mail addresses: dove.chen@msa.hinet.net (C.H. Chen), yk@cycu.edu.tw (Y. Kang).

0022-460X/$ - see front matter © 2006 Elsevier Ltd. All rights reserved.
doi:10.1016/j.jsv.2006.04.008

Nomenclature

A	effective recess area
a	axial flow land width
B_{ij}, $\bar{B}_{ij}$	damping coefficients, $\bar{B}_{ij} = B_{ij}c\omega/P_sLD$, $(i,j = x,y)$
c	radial clearance of bearing
D	journal diameter
d_c	diameter of capillary
d_o	diameter of orifice
e, ε	eccentricity, $\varepsilon = e/c$
e_o, ε_o	steady-state eccentricity, $\varepsilon_o = e_o/c$
e_p, ε_p	perturbed eccentricity, $\varepsilon_p = e_p/c$
F_x, F_y, $\bar{F}_x$, $\bar{F}_y$	fluid-film force components, $(\bar{F}_x, \bar{F}_y) = (F_x, F_y)/P_sLD$
h_o, $\bar{h}_o$	film thickness, $\bar{h}_o = h_o/c$
h_d, $\bar{h}_d$	recess depth at the downstream of restrictor inlet, $\bar{h}_d = h_d/c$
K_{ij}, $\bar{K}_{ij}$	stiffness coefficients, $\bar{K}_{ij} = K_{ij}c/P_sLD$ $(i,j = x,y)$
L	bearing length
$\overline{M}$	non-dimensional mass parameter, $\overline{M} = mc\omega^2/P_sLD$
$\overline{M}_c$	stability threshold, $\overline{M}_c = mc\omega_c^2/P_sLD$
m	rotor mass
P_d	pressure of downstream of restrictor inlet at the rth recess
P_o	static pressure
P_ε, P_ϕ	dynamic pressure
P_s	supply pressure
$\bar{P}$	non-dimensional pressure, P_a/P_s, subscript a denoted for P_o, P_r, P_ε and P_ϕ
Q_r	flow rate at the rth recess, $\bar{Q}_r = 12\mu Q_r/P_sc^3$
Q_{ro}	static flow rate
Q_ε, Q_ϕ	dynamic flow rate
$\bar{Q}$	non-dimensional flow rate, $\bar{Q}_b = 12\mu Q_b/P_sc^3$, subscript b denoted for Q_{ro}, Q_ε and Q_ϕ
R	journal radius
t	time coordinate
V_0, $\bar{V}_0$	recess volume, $\bar{V}_0 = V_0/Ac$
x, y, z, $\bar{x}$, $\bar{y}$, $\bar{z}$	Cartesian coordinates, $(\bar{x},\bar{y}) = (x,y)/c$, $\bar{z} = z/(L/2)$
W, $\overline{W}$	load capacity, $\overline{W} = W/P_sLD$
α	circumferential sill angle
β	fluid compressibility parameter
δ_c	capillary restriction parameter, $\delta_c = 3\pi d_c^4/32l_cc^3$
δ_o	orifice restriction parameter, $\delta_o = 3\sqrt{2}\pi\mu C_d d_o^2/\sqrt{\rho P_s c^3}$
ϕ_o	steady-state attitude angle
ϕ_p	perturbed attitude angle
γ	fluid compressibility parameter, $\gamma = \bar{V}_0\beta P_s$
Λ	speed parameter, $\Lambda = 6\mu\omega/P_s(c/R)^2$
λ	whirl ratio, $\lambda = \omega_p/\omega$
μ	absolute viscosity of lubricant
θ	angular coordinate
ρ	density of lubricant
σ	squeeze number, $\sigma = 6\mu\omega_p/P_s(c/R)^2$
τ	non-dimensional time, $\tau = \omega_p t$
ω	journal rotating speed
ω_c	critical journal rotating speed
ω_p	whirl frequency of journal center about the equilibrium point
ψ	frequency parameter, $\psi = \sigma A/R^2$

the laminar flow in journal bearing clearance by the simulation of utilizing two or three-dimensional Navier–Stokes equations. They obtained that the patterns of jet-dominated flow in both deep and shallow recesses are similar to each other. Therefore, Reynolds equation can be applied to the lubricant flow, which is jet-dominated in both sills and recesses.

Chen et al. [12,13] have determined the influences of restriction effects of capillary and orifice, respectively, on the stability of a rotor system supporting by deep or shallow recessed hybrid bearings. Their results have shown that restriction parameters dominate bearing load capacity and rotor stability, which provide appropriate selections of restriction parameters and land-width ratios in hybrid design for stability threshold.

This paper studies the restriction effects of capillary and orifice on the stability of a rigid rotor supported by hybrid bearings. The restriction influences are also compared with the same cases of hybrid bearing without restrictor. The stability threshold versus carrying load for various land-width ratios and various recess depth of the rigid rotor–hybrid bearing system are obtained from the analysis of load capacity and stability threshold, respectively, relative to the same eccentricity ratio.

2. Analysis

2.1. Lubrication equations of hybrid bearing

For an iso-viscous, incompressible lubricant situated in a hybrid bearing clearance assuming of laminar flow without inertial effect, the non-dimensional Reynolds equation of lubricant can be derived from Navier–Stokes equation and expressed in the Cartesian coordinates system as

$$\frac{\partial}{\partial\theta}\left(\bar{h}^3\frac{\partial\bar{P}}{\partial\theta}\right)+\left(\frac{D}{L}\right)^2\frac{\partial}{\partial\bar{z}}\left(\bar{h}^3\frac{\partial\bar{P}}{\partial\bar{z}}\right)=\Lambda\frac{\partial\bar{h}}{\partial\theta}+\sigma\frac{\partial\bar{h}}{\partial\tau}. \tag{1}$$

As shown in Fig. 1, the journal center rotates about its steady-state position (ε_o, ϕ_o) with a small whirl which is decomposed into radial and tangential components represented by $\mathrm{Re}(\varepsilon_p e^{i\tau})$ and $\mathrm{Re}(\varepsilon_o\phi_p e^{i\tau})$, respectively. This small journal whirl will induce small perturbations of the film pressure and film thickness which are composed of steady-state part subscripted by o and dynamic parts subscripted by ε and ϕ. Thus, the pressure and film thickness distributions can be expressed, respectively, by

$$\bar{P}=\bar{P}_o+\varepsilon_p e^{i\tau}\bar{P}_\varepsilon+\varepsilon_o\phi_p e^{i\tau}\bar{P}_\phi, \tag{2a}$$

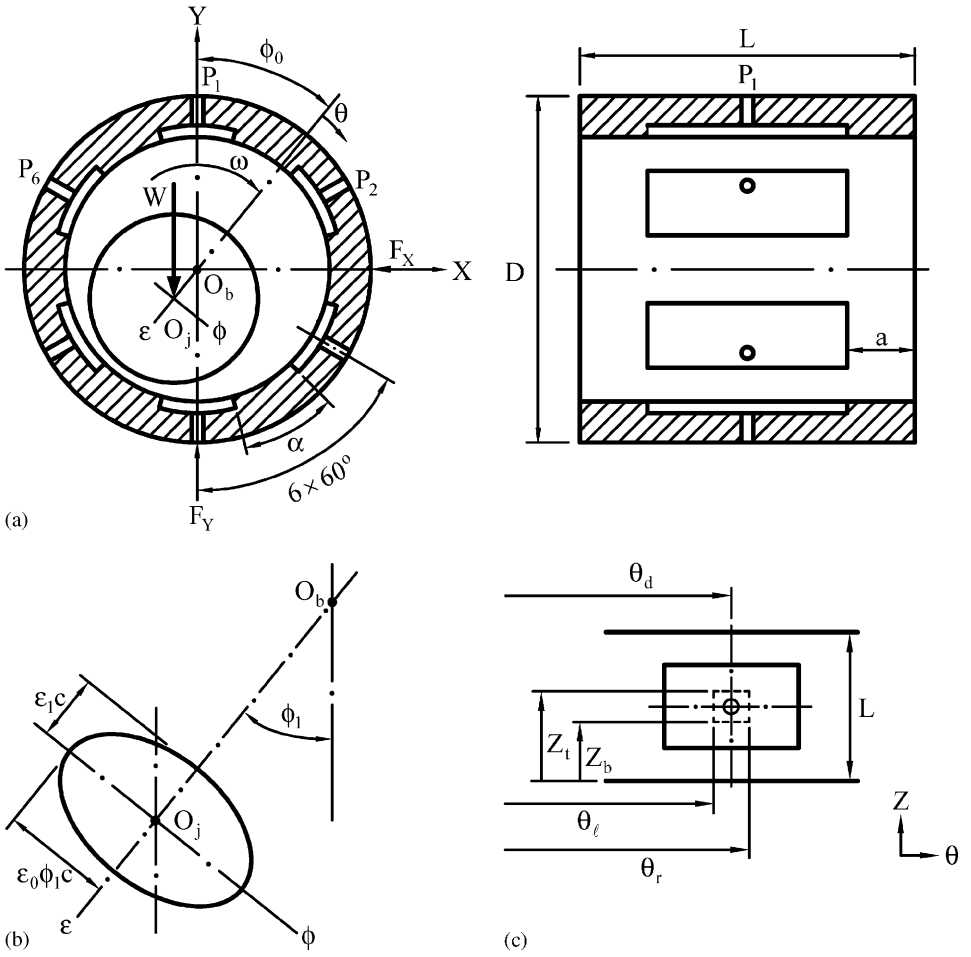

Fig. 1. Journal whirling in a six-recessed hybrid bearing: (a) configuration, (b) perturbed orbit of journal center, and (c) coordinates of recess edges.

$$\bar{h} = \bar{h}_o + \varepsilon_p e^{i\tau} \cos\theta + \varepsilon_o \phi_p e^{i\tau} \sin\theta. \tag{2b}$$

The perturbation method suggested by Ghosh et al. [6] is utilized substituting Eqs. (2a)–(2b) into Eq. (1) with neglecting higher order terms gives the linearized Reynolds equations of static and dynamic pressures. The details of these equations are shown in Ghosh et al. [6].

Pressure distribution within a shallow recess may vary as position changing. It can be seen from Braun and his colleagues [9–11] that pressure distribution in recess are strongly influenced by the jet strength, feed-line angle, aspect ratio, and recess depth. Since the boundary condition for downstream location of restrictor inlet must satisfy the pressure distribution, the appropriate boundary conditions for both shallow and deep recesses can be assumed as

(1) $\bar{P}_a(\theta, \bar{z} = \pm 1) = 0$ for both ends of a bearing;
(2) $\dfrac{\partial \bar{P}_a}{\partial \bar{z}}(\theta, \bar{z} = 0) = 0$ for the symmetry;
(3) $\bar{P}_a(\theta, \bar{z}) = \bar{P}_a(\theta + 2\pi, \bar{z})$ for the continuity of an intact film;
(4) $\bar{P}_a = \bar{P}_{da}$ for the downstream of restrictor inlet at the rth recess;
(5) $\bar{P}_a^+ = \bar{P}_a^-$ at adjacencies of recess and sill, where $+$ and $-$ denoted for sill and recess, respectively.

where a denoted for $\bar{P}_o$, $\bar{P}_\varepsilon$ and $\bar{P}_\phi$.

The linearized Reynolds equations with boundary conditions are solved numerically for static and dynamic pressure distributions by using the finite difference method, with a successive over-relaxation scheme.

The non-dimensional continuity equation of downstream flow of a restrictor at the rth recess for a hybrid bearing with capillary or orifice compensation can be given as

$$\delta(1 - \bar{P}_d)^m = \bar{Q}_r + \psi \frac{\partial}{\partial \tau}(\bar{h}_d), \tag{3}$$

where $m = 1$ and $\delta = \delta_c = 3\pi d_c^4 / 32 l_c c^3$ for a capillary restrictor and $m = 0.5$ and $\delta = \delta_o = 3\sqrt{2}\pi\mu C_d d_0^2 / \sqrt{\rho P_s} c^3$ for an orifice restrictor, $\psi = \sigma A / R^2$ and $\sigma = 6\mu\omega_p / P_s (c/R)^2$ are recess frequency parameter and squeeze number, respectively. The term on the left side of the equal sign refers to the mass flow into the recess through a restrictor, the first term on the right side of the equal sign is the mass flow out from the inlet of recess through the four edges of the rth recess, and the second terms refer to the time rate of mass changing due to squeeze effect. However, the compressible effect of lubricant is excluded from the continuity equation. For most conditions oil lubricants are considered to be incompressible because of low frequency of dynamic loading and the relatively small volume of oil in the recesses and between recess and the restrictor. However, at high frequencies, the compressibility becomes significant effect of reducing the dynamic stiffness and damping of a bearing film.

Also, the perturbations of $\bar{P}_d$, $\bar{h}_d$ and $\bar{Q}_r$ are expressed as

$$\bar{P}_d = \bar{P}_{do} + \varepsilon_p e^{i\tau} \bar{P}_{d\varepsilon} + \varepsilon_o \phi_p e^{i\tau} \bar{P}_{d\phi}, \tag{4a}$$

$$\bar{h}_d = \bar{h}_{do} + \varepsilon_p e^{i\tau} \cos\theta_d + \varepsilon_o \phi_p e^{i\tau} \sin\theta_d, \tag{4b}$$

$$\bar{Q}_r = \bar{Q}_{ro} + \varepsilon_p e^{i\tau} \bar{Q}_\varepsilon + \varepsilon_o \phi_p e^{i\tau} \bar{Q}_\phi, \tag{4c}$$

where θ_d is the angular position of the downstream of restrictor inlet.

The expression for the outflow of lubricant from the recess is given by

$$\begin{aligned}\bar{Q}_r = &\int_{\theta_l}^{\theta_r} \left(-\bar{h}_d^3 \frac{\partial \bar{P}}{\partial \bar{z}} \right)_{\bar{z}=\bar{z}_b} \mathrm{d}\theta + \int_{\bar{z}_b}^{\bar{z}_t} \left(\Lambda \bar{h}_d - \bar{h}_d^3 \frac{\partial \bar{P}}{\partial \theta} \right)_{\theta=\theta_l} \mathrm{d}\bar{z} \\ &+ \int_{\theta_l}^{\theta_r} \left(-\bar{h}_d^3 \frac{\partial \bar{P}}{\partial \bar{z}} \right)_{\bar{z}=\bar{z}_t} \mathrm{d}\theta + \int_{\bar{z}_b}^{\bar{z}_t} \left(\Lambda \bar{h}_d - \bar{h}_d^3 \frac{\partial \bar{P}}{\partial \theta} \right)_{\theta=\theta_r} \mathrm{d}\bar{z},\end{aligned} \tag{5}$$

where θ_1 and θ_r are referred to both bounds of circumferential coordinates and $\bar{z}_b$ and $\bar{z}_t$ are referred to both bounds of axial coordinates, respectively, of the downstream edges of restrictor inlet at the rth recess as shown

in Fig. 1(c). Similarly, the static and dynamic pressures of downstream of restrictor inlet in recesses can be obtained by substituting Eqs. (4a)–(4c) into Eqs. (3) and (5), and equating coefficients of static and dynamic perturbations on both sides gives

$$\bar{P}_{do} = 1 - \left(\frac{\bar{Q}_{ro}}{\delta}\right)^{\zeta}, \tag{6}$$

$$\bar{P}_{d\varepsilon} = -\frac{\left(2\sqrt{1-\bar{P}_{do}}\right)^{\eta}}{\delta}(\bar{Q}_{\varepsilon} + i\psi\cos\theta_d), \tag{7}$$

$$\bar{P}_{d\phi} = -\frac{\left(2\sqrt{1-\bar{P}_{do}}\right)^{\eta}}{\delta}(\bar{Q}_{\phi} + i\psi\sin\theta_d), \tag{8}$$

where $\zeta = 1$ and $\eta = 0$ for capillary restriction, and $\zeta = 2$ and $\eta = 1$ for orifice restriction.

2.2. Load capacity

The bearing load capacity is equivalent to reactive resistances which are induced by fluid film pressure in the bearing clearance. The non-dimensional components of the resultant reaction forces can be obtained by

$$\bar{F}_x = \frac{F_x}{P_s LD} = -2\int_0^1\int_0^{2\pi}\bar{P}_o\cos\theta\,\mathrm{d}\theta\,\mathrm{d}\bar{z}, \tag{9a}$$

$$\bar{F}_y = \frac{F_y}{P_s LD} = -2\int_0^1\int_0^{2\pi}\bar{P}_o\sin\theta\,\mathrm{d}\theta\,\mathrm{d}\bar{z}. \tag{9b}$$

Hence, the non-dimensional load capacity is given by

$$\overline{W} = \sqrt{\bar{F}_x^2 + \bar{F}_y^2}. \tag{10}$$

2.3. Stiffness and damping coefficients

The non-dimensional stiffness and damping coefficients along the ε and ϕ directions due to the dynamic pressures $\bar{P}_{\varepsilon}$ and $\bar{P}_{\phi}$ can be determined by

$$\begin{bmatrix}\bar{K}_{\varepsilon\varepsilon} & K_{\phi\phi}\\ \bar{K}_{\phi\varepsilon} & \bar{K}_{\varepsilon\phi}\end{bmatrix} = -\mathrm{Re}\left\{2\int_0^1\int_0^{2\pi}\begin{bmatrix}\cos\theta & \sin\theta\\ \sin\theta & \cos\theta\end{bmatrix}\begin{bmatrix}\bar{P}_{\varepsilon} & 0\\ 0 & \bar{P}_{\phi}\end{bmatrix}\mathrm{d}\theta\,\mathrm{d}\bar{z}\right\}, \tag{11}$$

$$\begin{bmatrix}\bar{B}_{\varepsilon\varepsilon} & \bar{B}_{\phi\phi}\\ \bar{B}_{\phi\varepsilon} & \bar{B}_{\varepsilon\phi}\end{bmatrix} = -\mathrm{Im}\left\{2\int_0^1\int_0^{2\pi}\begin{bmatrix}\cos\theta & \sin\theta\\ \sin\theta & \cos\theta\end{bmatrix}\begin{bmatrix}\bar{P}_{\varepsilon} & 0\\ 0 & \bar{P}_{\phi}\end{bmatrix}\mathrm{d}\theta\,\mathrm{d}\bar{z}\right\}, \tag{12}$$

where $\bar{B}_{ij} = B_{ij}c\omega/P_s LD$ and, $\bar{K}_{ij} = K_{ij}c/P_s LD, (i,j = \varepsilon,\phi)$.

Using coordinate transformation the non-dimensional stiffness and damping coefficients along the x and y directions can be obtained from

$$\begin{bmatrix}\bar{K}_{xx} & \bar{K}_{xy}\\ \bar{K}_{yx} & \bar{K}_{yy}\end{bmatrix} = \begin{bmatrix}\cos\phi_0 & -\sin\phi_0\\ \sin\phi_0 & \cos\phi_0\end{bmatrix}\begin{bmatrix}\bar{K}_{\varepsilon\varepsilon} & \bar{K}_{\varepsilon\phi}\\ \bar{K}_{\phi\varepsilon} & \bar{K}_{\phi\phi}\end{bmatrix}\begin{bmatrix}\cos\phi_0 & \sin\phi_0\\ -\sin\phi_0 & \cos\phi_0\end{bmatrix}, \tag{13}$$

$$\begin{bmatrix}\bar{B}_{xx} & \bar{B}_{xy}\\ \bar{B}_{yx} & \bar{B}_{yy}\end{bmatrix} = \begin{bmatrix}\cos\phi_0 & -\sin\phi_0\\ \sin\phi_0 & \cos\phi_0\end{bmatrix}\begin{bmatrix}\bar{B}_{\varepsilon\varepsilon} & \bar{B}_{\varepsilon\phi}\\ \bar{B}_{\phi\varepsilon} & \bar{B}_{\phi\phi}\end{bmatrix}\begin{bmatrix}\cos\phi_0 & \sin\phi_0\\ -\sin\phi_0 & \cos\phi_0\end{bmatrix}. \tag{14}$$

where ϕ_o is the steady-state attitude angle.

2.4. Stability threshold of rigid rotor–hybrid bearing system

In the fixed reference coordinates (O_b, x, y) a rigid rotor is supported horizontally by two identical hybrid journal bearings. The rotor is assumed to consist of a massless shaft and a single, centered mass m without unbalance mass as illustrated in Fig. 2. When the journal is operating in its steady state at the conditions of a given load capacity W, lubricant viscosity μ, supply pressure P_s and shaft speed ω, for a small disturbance in film pressure the non-dimensional perturbation equations of center motion of the rigid rotor with whirl frequency ω_p about the equilibrium position can be expressed by

$$\overline{M}\lambda^2 \frac{\mathrm{d}^2\bar{x}}{\mathrm{d}\tau^2} = -2\bar{F}_x = -2(\bar{K}_{xx}\bar{x} + \bar{K}_{xy}\bar{y} + \lambda\bar{B}_{xx}\dot{\bar{x}} + \lambda\bar{B}_{xy}\dot{\bar{y}}), \tag{15}$$

$$\overline{M}\lambda^2 \frac{\mathrm{d}^2\bar{y}}{\mathrm{d}\tau^2} = -2\bar{F}_y = -2(\bar{K}_{yx}\bar{x} + \bar{K}_{yy}\bar{y} + \lambda\bar{B}_{yx}\dot{\bar{x}} + \lambda\bar{B}_{yy}\dot{\bar{y}}), \tag{16}$$

where $\overline{M} = mc\omega^2/P_sLD$ is mass parameter, $\lambda = \omega_p/\omega$ is whirl ratio, and components of bearing force, along with the stiffness and damping coefficients, are determined by integration of static and dynamic pressures, respectively, as mentioned above.

Substituting $\bar{x} = \bar{X}e^{s\tau}$ and $\bar{y} = \bar{Y}e^{s\tau}$, where $\bar{X}$ and $\bar{Y}$ are constant, into Eqs. (15) and (16) gives a set of simultaneous and linear equations of $\bar{X}$ and $\bar{Y}$. The value of coefficients determinant of the linear equations set must be zero for non-trivial solutions of $\bar{X}$ and $\bar{Y}$. Thus, the characteristic equation of complex eigenvalues for this rigid rotor–hybrid bearing system is obtained in the form of an algebraic polynomial of s with the coefficients being functions of stiffness and damping coefficients. According to Routh–Hurwitz theory, the stability threshold of this system can be determined by

$$\overline{M}_c = \frac{mc\omega_c^2}{P_sLD} = \frac{2A_1A_3A_5}{A_1^2 + A_2A_5^2 - A_1A_4A_5}, \tag{17}$$

where $A_1 = \bar{K}_{xx}\bar{B}_{yy} + \bar{K}_{yy}\bar{B}_{xx} - \bar{K}_{xy}\bar{B}_{yx} - \bar{K}_{yx}\bar{B}_{xy}$, $A_2 = \bar{K}_{xx}\bar{K}_{yy} - \bar{K}_{xy}\bar{K}_{yx}$, $A_3 = \bar{B}_{xx}\bar{B}_{yy} - \bar{B}_{xy}\bar{B}_{yx}$, $A_4 = \bar{K}_{xx} + \bar{K}_{yy}$ and $A_5 = \bar{B}_{xx} + \bar{B}_{yy}$ as seen in Ref. [12].

Consequently, the instability induced by self-excited vibration occurs when value $\overline{M}$ of this system is larger than $\overline{M}_c$. Conversely, for $\overline{M} < \overline{M}_c$, the vibration resulting from initial perturbation of the rotor dies out exponentially with time. Thus, $\overline{M} = \overline{M}_c$ relates to the critical condition at which the rotor whirls to a limit cycle through transient vibration.

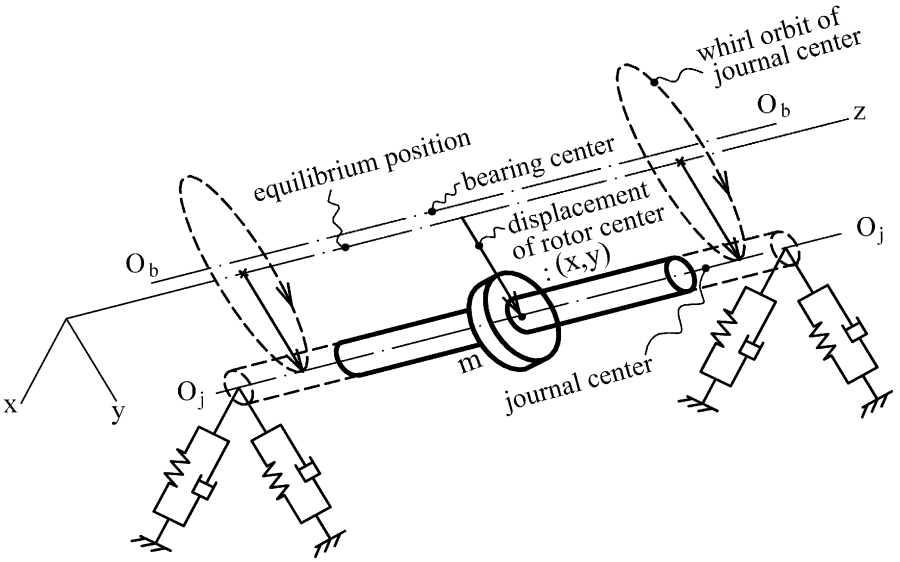

Fig. 2. Rigid rotor model.

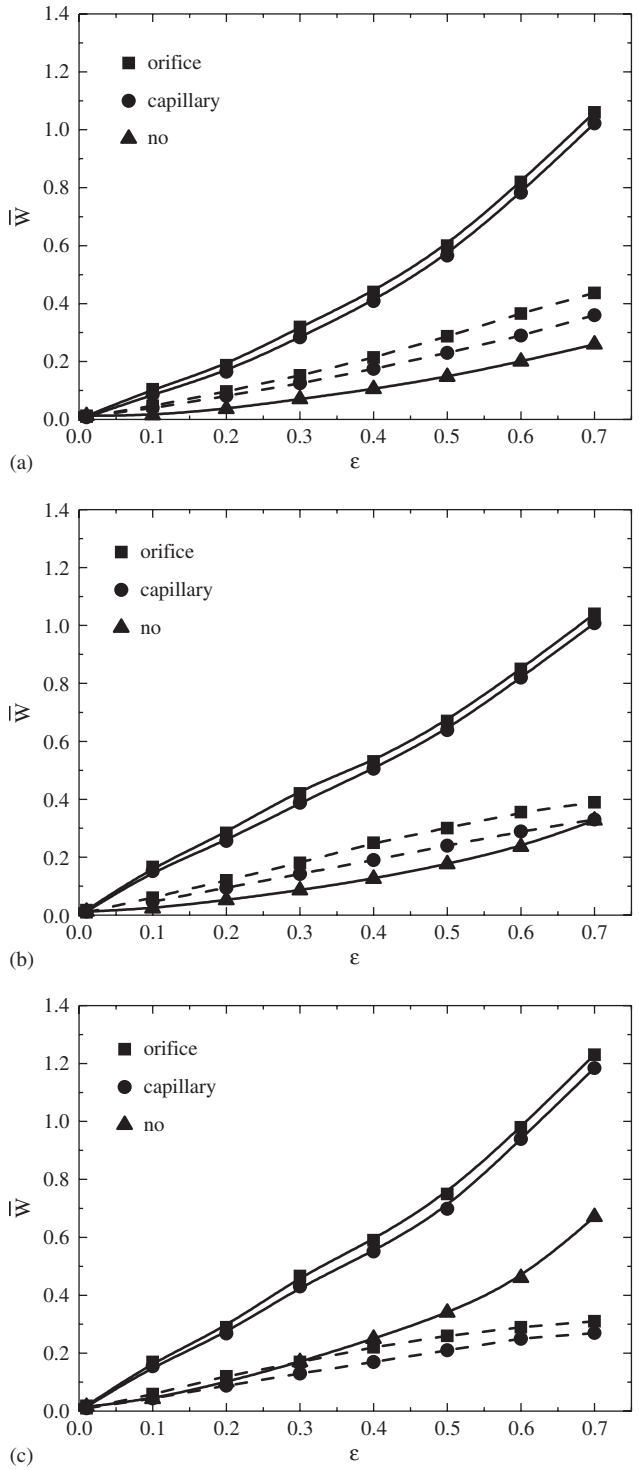

Fig. 3. The load capacity $(\overline{W})$ of shallow-recessed bearing ($h_d = c = 1.0$) versus eccentricity ratio (ε) for: (a) $a/L = 0.1$, (b) $a/L = 0.25$, (c) $a/L = 0.4$, ——— for $\Lambda = 6.0$, – – – for $\Lambda = 0.0$.

3. Results and discussion

This study has analyzed the dynamic characteristics of a rigid rotor–hybrid bearing system rotating with $\Lambda = 6.0$ or non-rotating with $\Lambda = 0.0$. The rigid rotor is supported by two single-row and six-recessed hybrid bearings, which are regulated by capillary and orifice or without using restrictors, respectively. According to simulation results in Chen et al. [12,13] both restriction parameters of capillary and orifice are selected as $\delta_c = \delta_o = 2.0$, which can yield good stability. The bearing geometric parameters are selected as $L/D = 1.0$ and $\alpha = 34^\circ$. For three land-width ratios ($a/L = 0.1$, 0.25 and 0.4) simulations of load capacity $(\overline{W})$ and stability threshold $(\overline{M}_c)$ for both shallow ($h_d = c = 1.0$) and deep ($h_d = c = 5.0$) recesses are described as follows.

3.1. Comparison of the restriction effects

The variations of load capacity $(\overline{W})$ and stability threshold $(\overline{M}_c)$ versus eccentricity ratio (ε) of shallow-recessed bearing with three land-width ratios cases are shown in Figs. 3 and 4, respectively. It can be found that for all cases, the orifice compensated bearings are better from the point of view of support than capillary compensated bearings. Also, the $\overline{W}$ is increased with an increase of speed parameter (Λ) owing to the increase of hydrodynamic effects.

For $\Lambda = 6.0$, the $\overline{W}$ increases with an increase of land-width ratio (a/L) due to the predominance of hydrodynamic effect get over hydrostatic effect. However, it is contrary to $\Lambda = 0.0$, since increase of land-width ratio results in decreasing of hydrostatic effect, which is dominance of hydrostatic load capacity.

It is observed that for all cases the orifice compensated bearings provide larger stability threshold than capillary compensated bearings. This superiority may be attributed to the conclusion of Cheng and Rowe [8], who have revealed that orifice may give fractionally greater stiffness. The influence of land-width ratio on stability is contrary to load capacity; the stability threshold gets larger as land-width ratio decreasing.

For cases with three land-width ratios the variations of load capacity $(\overline{W})$ and stability threshold $(\overline{M}_c)$ versus eccentricity ratio (ε) of deep-recessed bearing are shown in Figs. 5 and 6, respectively. It is observed that for all cases, the comparative results of restriction effect, land-width ratio and speed parameter on both load capacity $(\overline{W})$ and stability threshold $(\overline{M}_c)$ are similar to those cases of shallow-recessed bearing.

For $\Lambda = 6.0$ the $\overline{W}$ of deep-recessed bearing is smaller than that of shallow-recessed bearing for the same land-width ratio since the shallow recesses can provide more hydrodynamic pressures than deep recesses. Contrarily, for $\Lambda = 0.0$ the $\overline{W}$ of deep-recessed bearing is larger than that of shallow-recessed bearing for the same land-width ratio, since the deep recesses can provide more hydrostatic pressures than shallow recesses.

For large eccentricity ratio the $\overline{M}_c$ of deep-recessed bearing is smaller than that of shallow-recessed bearing, this is because of that the hydrodynamic effects are generated not only in lands but also in shallow recesses. While, for small eccentricity ratio the coupled hydrostatic and hydrodynamic effects are provided by shallow recesses which may induce a smaller $\overline{M}_c$, therefore, the $\overline{M}_c$ of deep-recessed bearing is superior to that of shallow-recessed bearing.

For cases with three land-width ratios the variations of stability threshold $(\overline{M}_c)$ versus carrying load $(\overline{W})$ are drawn in Fig. 7. According to above descriptions it can be found that from the viewpoint of stability, there exists a critical point of carrying loads for both capillary and orifice, when the carrying load is greater than this point the bearings should be designed with shallow recesses, otherwise, the deep recesses are requisite.

For three land-width ratios $a/L = 0.1$, 0.25 and 0.4 cases, the critical point of carrying loads for orifice are $\overline{W} = 0.4$, 0.55 and 0.9, respectively, and for capillary are $\overline{W} = 0.5$, 0.7 and 0.95, respectively. Obviously, the values of critical point are increased with the increase of land-width ratio. And, this point of orifice occurs earlier than that of capillary.

3.2. Comparison in dynamic pressures with or without considering recess volume compressibility

When the recess volume compressibility effect in the bearing recesses and downstream of restrictors inlet is taken into consideration, $\psi\gamma(\partial\bar{P}_d/\partial\tau)$ is added in the right side on the equal sign of Eq. (3). This term describes the time rate of mass changing in recesses as the lubricant subjected to compressive deformation, where fluid compressibility parameter is defined by $\gamma = \overline{V}_0\beta P_s$ and $\overline{V}_0$ is non-dimensional lubricant volume of recess.

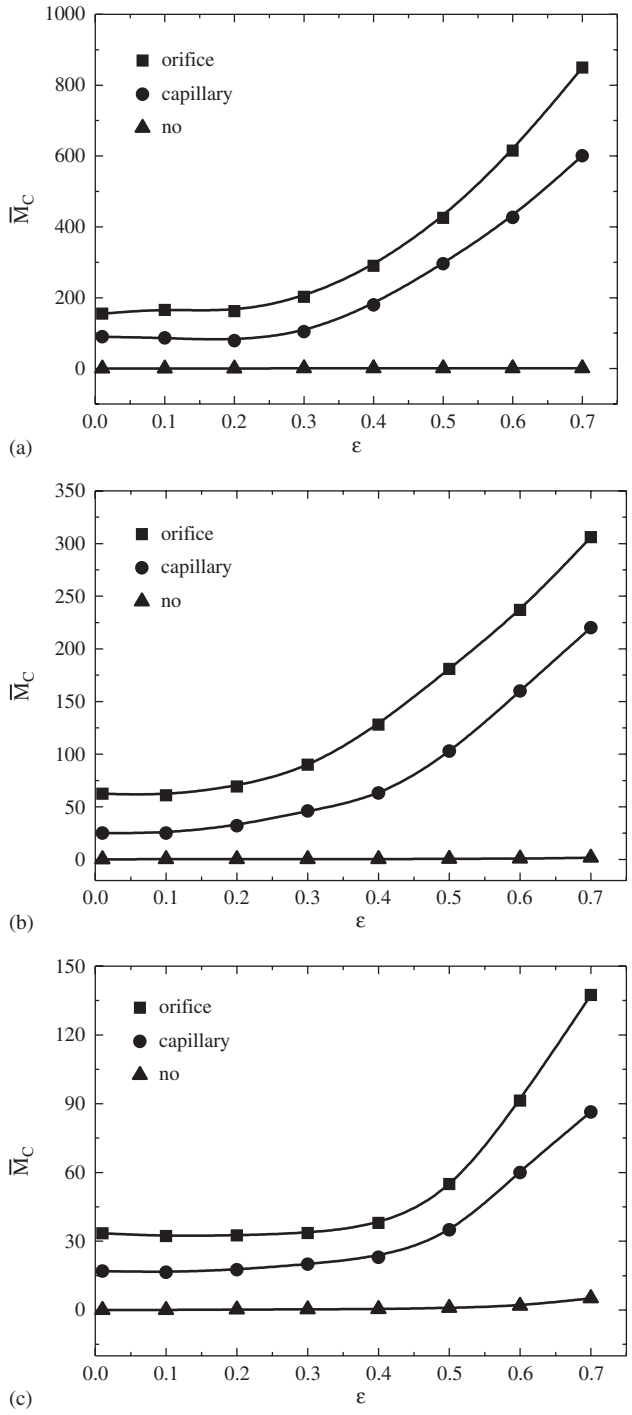

Fig. 4. The stability threshold $(\overline{M}_c)$ versus eccentricity ratio (ε) of the rotor rotating at $\Lambda = 6.0$ and supported by shallow-recessed bearings for: (a) $a/L = 0.1$, (b) $a/L = 0.25$, and (c) $a/L = 0.4$.

Consequently, the dynamic pressures $\overline{P}_{d\varepsilon}$ and $\overline{P}_{d\phi}$ are added by the compressibility effect terms in both real and image parts after the same procedures of substituting Eqs. (4a)–(4c) into the modified continuity equation which is Eq. (3) added by compressibility effect term $\psi\gamma(\partial\bar{P}_d/\partial\tau)$.

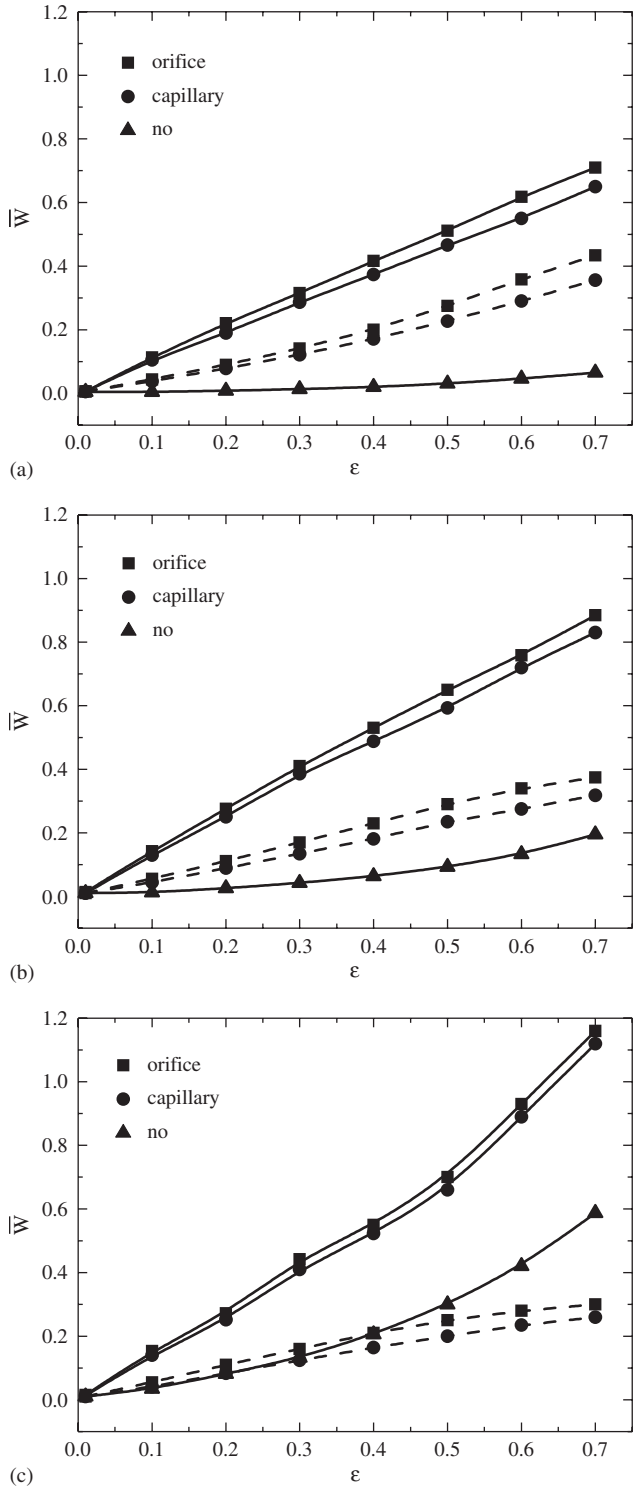

Fig. 5. The load capacity $(\overline{W})$ of deep-recessed bearing ($h_d = c = 5.0$) versus eccentricity ratio (ε) for: (a) $a/L = 0.1$, (b) $a/L = 0.25$, and (c) $a/L = 0.4$, ——— for $\Lambda = 6.0$, – – – for $\Lambda = 0.0$.

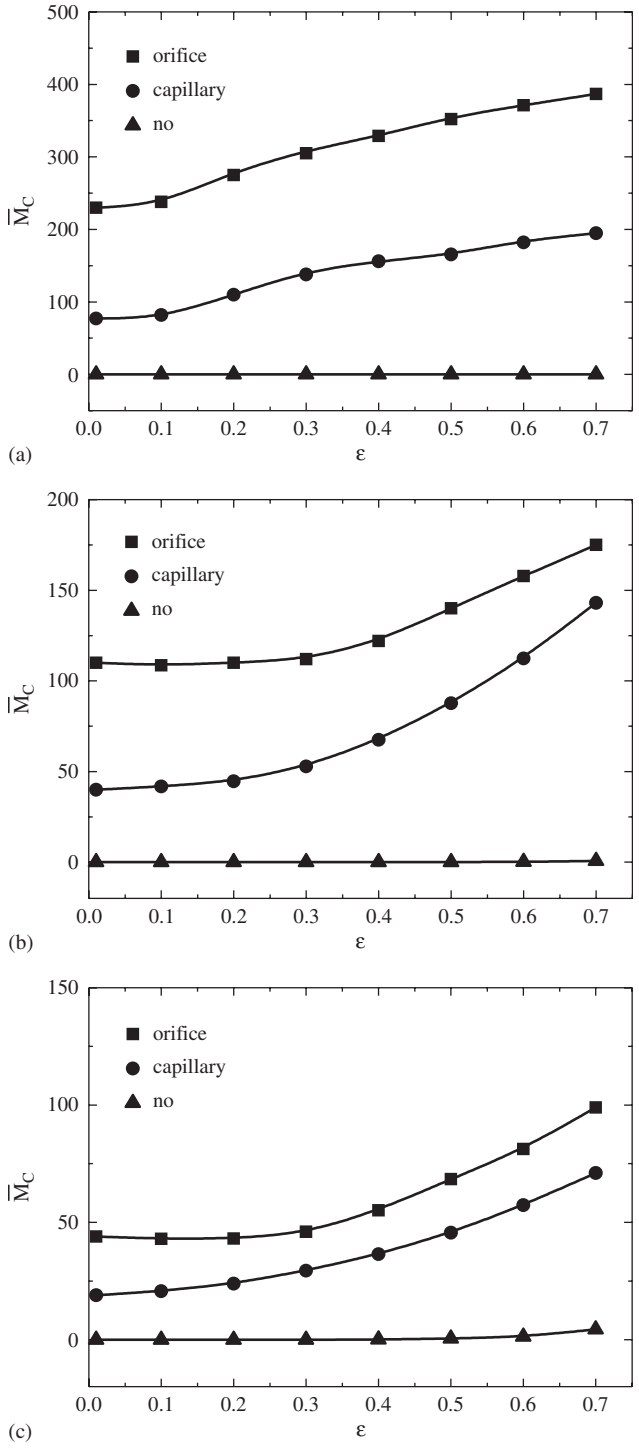

Fig. 6. The stability threshold $(\overline{M}_c)$ versus eccentricity ratio (ε) of the rotor rotating at $\Lambda = 6.0$ and supported by deep-recessed bearings for: (a) $a/L = 0.1$, (b) $a/L = 0.25$, and (c) $a/L = 0.4$.

The influences of recess compressibility in changing of dynamic pressures $\overline{P}_{d\varepsilon}$ and $\overline{P}_{d\phi}$ have been evaluated for numerical examples of this paper and listed in Table 1. for the comparisons of the continuity equation with or without compressibility effect. The results show that for both deep and shallow recesses with capillary or

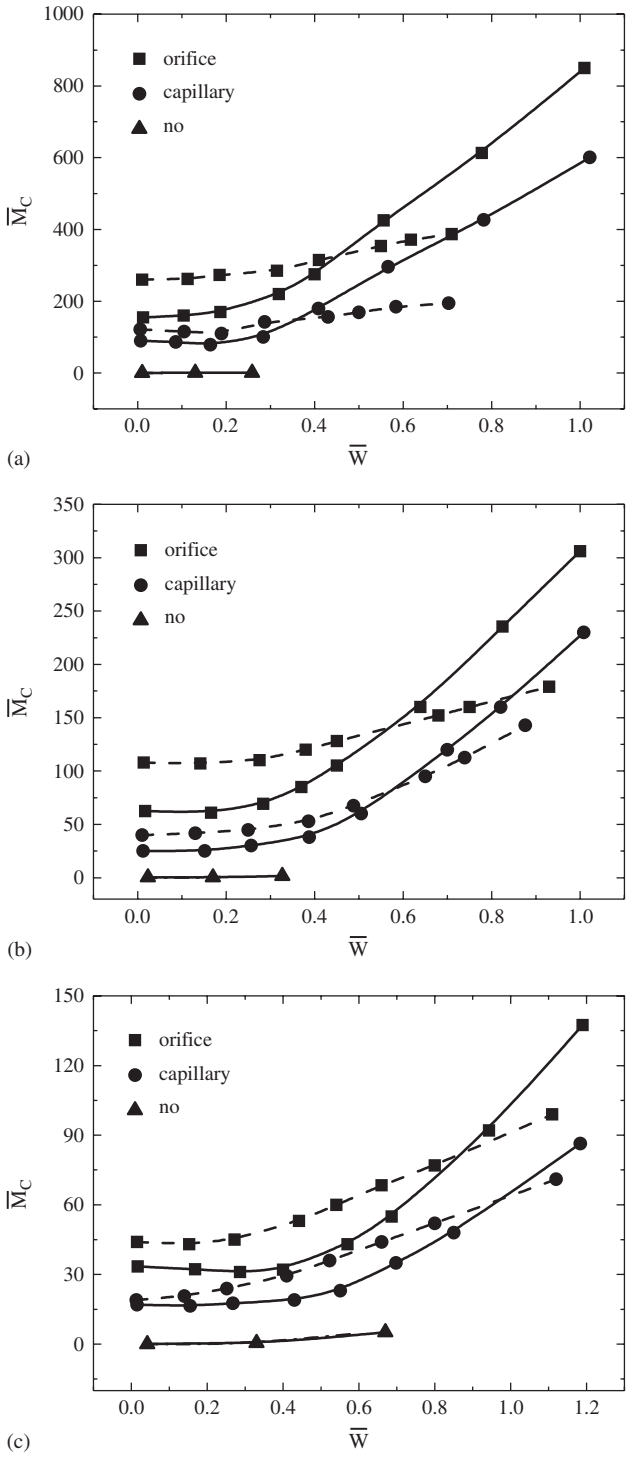

Fig. 7. The stability threshold $(\overline{M}_c)$ versus carrying load $(\overline{W})$ of the rotor rotating at $\Lambda = 6.0$ for: (a) $a/L = 0.1$, (b) $a/L = 0.25$, and (c) $a/L = 0.4$, ——— for $h_d = c = 1.0$, — — — for $h_d = c = 5.0$.

orifice cases the reducing percentages of absolute values of dynamic pressures $\overline{P}_{d\varepsilon}$ and $\overline{P}_{d\phi}$ are all less than 3%. Therefore, in this paper, the recess compressible effect is neglected and the term $\psi\gamma(\partial\bar{P}_d/\partial\tau)$ is excluded from the continuity equation.

Table 1
Recess compressibility effect in dynamic pressures

Recess type	δ	γ	ψ	Reducing percentage of absolute values of maximum pressure $\bar{P}_{r\varepsilon}$ & $\bar{P}_{r\phi}$
Orifice restriction				
$h_d = c = 5$	2.0	2.5×10^{-3}	60	−0.74%−2.89%
$h_d = c = 1$	2.0	5×10^{-4}	60	−1.13%−0.878%
Capillary restriction				
$h_d = c = 5$	2.0	2.5×10^{-3}	60	−0.49% + 0.07%
$h_d = c = 1$	2.0	5×10^{-4}	60	−0.164% + 0.007%

4. Conclusion

The influences of restriction effects of capillary and orifice on the stability of a rigid rotor supported by hybrid bearings are studied by Routh–Hurwitz method. The simulation results are concluded as:

(1) The orifice compensated bearings are better from the point of view of support than capillary compensated bearings.
(2) For both shallow- and deep-recessed hybrid bearings at $\Lambda = 6.0$, the load capacities are increased with an increase of land-width ratio. Contrarily, for $\Lambda = 0.0$ the load capacities are increased with a decrease of land-width ratio.
(3) For all cases the bearings with orifice restriction can provide larger stability threshold than with capillary for a rigid rotor subjected to a specific carrying load.
(4) For stability of large carrying load the shallow-recessed bearings are superior to the deep-recessed bearings. Contrarily, for stability of small carrying load the deep-recessed bearings are superior to the shallow-recessed bearings.
(5) Thus, from the view for stability in bearing design with either capillary or orifice, when the carrying load exceed its critical point the bearing should be designed with shallow recesses, otherwise, the deep recesses are requisite in order to obtain appreciate stability threshold for a rigid rotor–hybrid bearing system.

References

[1] A.A. Raimondi, J. Boyd, An analysis of orifice- & capillary-compensated hydrostatic journal bearings, *Journal of the American Society of Lubrication Engineering* 13 (1) (1957) 29–37.
[2] W.B. Rowe, F.S. Chong, Computation of dynamic force coefficients for hybrid (hydrostatic/hydrodynamic) journal bearings by the finite disturbance and perturbation techniques, *Tribology International* 19 (5) (1986) 260–271.
[3] M.K. Ghosh, Dynamic characteristic of multirecess externally pressurized oil journal bearing, *Transactions of the ASME, Journal of Lubrication Technology* 100 (3) (1978) 467–471.
[4] M.K. Ghosh, B.C. Majumdar, J.S. Rao, Steady state and dynamic behavior of multi-recess hybrid oil journal bearings, *Journal of Mechanical Engineering Science* 21 (5) (1979) 345–451.
[5] M.K. Ghosh, N.S. Viswanath, Recess volume fluid compressibility effect on the dynamic characteristics of multirecess hydrostatic journal bearings with journal rotation, *Transactions of the ASME, Journal of Tribology* 109 (3) (1987) 417–426.
[6] M.K. Ghosh, S.K. Guha, B.C. Majumdar, Rotordynamic coefficients of multirecess hybrid journal bearings part I, *Wear* 129 (2) (1989) 245–259.
[7] S.K. Guha, M.K. Ghosh, B.C. Majumdar, Rotordynamic coefficients of multirecess hybrid journal bearings part II: fluid inertia effect, *Wear* 129 (2) (1989) 261–272.
[8] K. Cheng, W.B. Rowe, A selection strategy for the design of externally pressurized journal bearings, *Tribology International* 28 (7) (1995) 465–474.
[9] M.J. Braun, F.K. Choy, Y.M. Zhou, The effects of a hydrostatic pocket aspect ratio, supply orifice position, and attack angle on steady-state flow patterns, pressure, and shear characteristics, *Journal of Tribology, Transactions of the ASME* 115 (4) (1993) 678–685.

[10] M.J. Braun, M.B. Dzodzo, Effects of the feedline and the hydrostatic pocket depth on the flow pattern and pressure distribution, *Journal of Tribology, Transactions of the ASME* 117 (2) (1995) 224–233.
[11] M.J. Braun, M.B. Dzodzo, Three-dimensional flow and pressure patterns in a hydrostatic journal bearing pocket, *Journal of Tribology, Transactions of the ASME* 119 (4) (1997) 711–719.
[12] C.H. Chen, Y. Kang, Y.N. Huang, C.H. Chu, J.T. Teng, The restrictive effects of capillary compensation on the stability of the Jeffcott rotor–hybrid bearing system, *Tribology International* 35 (12) (2002) 849–855.
[13] C.H. Chen, Y. Kang, C.C. Huang, The influences of orifice restriction and journal eccentricity on the stability of the rigid rotor–hybrid bearing system, *Tribology International* 37 (3) (2003) 227–234.